THE JOURNAL OF PHYSICAL CHEMISTRY C

Article

pubs.acs.org/JPCC

Theoretical Study of Phase Separation of Scandium Hydrides under High Pressure

Xiaoqiu Ye,[†,§] Roald Hoffmann,*[,†] and N. W. Ashcroft[‡]

[†]Department of Chemistry and Chemical Biology and [‡]Laboratory of Atomic and Solid Physics, Cornell University, Ithaca, New York 14853, United States

[§]China Academy of Engineering Physics, Mianyang, Sichuan 621900, China

Supporting Information

ABSTRACT: We report theoretical calculations of the static ground-state structures and pressure-induced phase transformations of three scandium hydrides: ScH, ScH_2, and ScH_3. For the monohydride, ScH, we predict several phases to be more stable at 1 atm than the previously suggested rock-salt structure, in particular one of $P4_2/mmc$ symmetry. The NaCl-type structure for ScH takes over at 10 GPa and dominates over a wide pressure range until it is replaced by a *Cmcm* structure around 265 GPa. Under pressure, the experimental P = 1 atm CaF_2-type structure of ScH_2 should transform to a $C2/m$ structure around 65 GPa, which then is likely to disproportionate to NaCl-type ScH and face-centered cubic ScH_3 above 72 GPa. According to theory, as the pressure is elevated, ScH_3 moves through the following sequence of phases: $P6_3 \rightarrow Fm\bar{3}m \rightarrow P6_3/mmc$($YH_3$-type) $\rightarrow$ *Cmcm*; the corresponding transition pressures are calculated to be 29, 360, and 483 GPa, respectively. The predicted disproportionation tendencies of ScH_2 are fascinating: stable to decomposition to ScH and ScH_3 at low pressures, it should begin to disproportionate near 72 GPa. However, the process is predicted to reverse at still higher pressures (above 300 GPa). We also find ScH to be stable to disproportionation to Sc and ScH_2 above ~25 GPa. The three hydrides are metallic, except for (at low pressures) ScH_3.

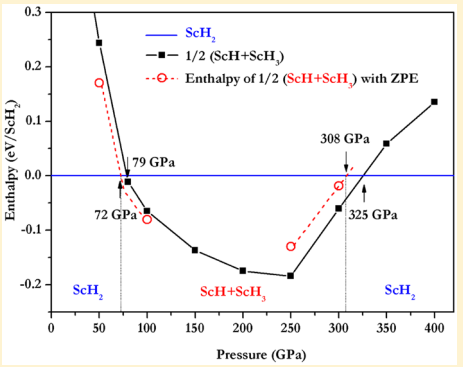

INTRODUCTION

Interest in the hydrides of scandium derives from their potential for hydrogen storage[1−3] as well as their intriguing and complex structural, electronic, and vibrational properties.[1,2] In this paper we begin a thorough theoretical exploration of the hydrides of element no. 21, at the beginning of the first transition series, across a wide pressure range.

Similar to other group III metals, yttrium (Y), lanthanum (La), and most rare earths, scandium (Sc) at hydrogen pressures well below 1 atm forms a dihydride whose CaF_2-type crystal structure (Figure 1, left) has all hydrogens occupying the tetrahedral holes of a face-centered cubic (fcc) lattice.[3] Given that the normal oxidation state of Sc is 3+, one would expect the ready formation of a trihydride. However, experimentally the synthesis of scandium trihydride by the reaction of Sc powder and hydrogen requires pressure greater than 0.3 GPa,[1] while trihydrides of other metals form at low hydrogen pressures. Samples of ScH_3 formed at elevated pressure are thermally unstable on return to P = 1 atm and T = 300 K, and nonstoichiometry is common.[4]

Nevertheless, a solid-state structure, including hydrogen positions, has been recently determined by neutron diffraction on a near-stoichiometric $ScH_{2.9}$ crystal.[1] The idealized structure assumed by the scandiums is hexagonal close packed (hcp), space group $P6_3/mmc$. The octahedral (O) sites of the hydrogen atoms are split into two, positioned near the metal basal plane (Figure 1, right, both sites are shown by the hydrogen atoms in blue and white color). The O-site hydrogen atoms randomly occupy one of the two equivalent positions, in contrast to YH_3, in which the proton positions are ordered.[5]

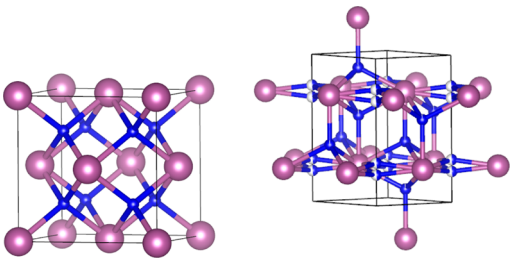

Figure 1. Experimental (P = 1 atm and room temperature) structures of the better known scandium hydrides; see text for details. (Left) ScH_2 in the $Fm\bar{3}m$ CaF_2 structure type. (Right) Idealized $P6_3/mmc$ structure of ScH_3. Two sites are shown for each H atom, each half-blue, half-white; only one of these is occupied. Purple balls are Sc, blue hydrogen.

Experimentally, when scandium hydrides are synthesized by hydrogenation of a scandium foil with hydrogen under high

Received: December 16, 2014
Revised: February 10, 2015
Published: February 12, 2015

Downloaded by CORNELL UNIV on September 8, 2015 | http://pubs.acs.org
Publication Date (Web): February 27, 2015 | doi: 10.1021/jp512538e

ACS Publications © 2015 American Chemical Society

DOI: 10.1021/jp512538e
J. Phys. Chem. C 2015, 119, 5614−5625

pressure and at standard temperature, ScH_3 (slightly off stoichiometry) starts to appear at 5.3 GPa (the 0.3 GPa cited earlier is for a synthesis using Sc powder), then transforms sluggishly into another phase in the 25−45.9 GPa range.[2] The structure of that intermediate phase has not been clearly identified. At pressures higher than 30 GPa, ScH_3 begins to transform to an fcc structure (of the Sc atoms) (Figure 2, left).[2]

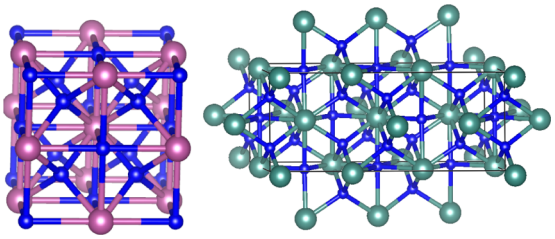

Figure 2. Experimental room-temperature structures of ScH_3 and YH_3 at 25 GPa; see text for degree of certainty of these. (Left) The $Fm\bar{3}m$ structure of ScH_3. (Right) The $C2/m$ structure of YH_3. Purple balls are Sc, green Y, blue hydrogen.

In a study of the related YH_3, a structure intermediate between hcp and fcc was found and classified as $C2/m$ (Figure 2, right).[6] For ScH_3 it was suggested that the transition from the hcp to the fcc heavy atom lattice follows a Cm symmetry continuous path.[7] We will describe these two paths and the intermediate structures in detail below.

A monohydride, ScH, appears to exist, but little information is available on it. Machida et al.[8] observed the formation of a NaCl-type monodeuteride of lanthanum, LaD, by the disproportionation of LaD_2 around 11 GPa. This paper reports briefly on similar pressure-induced reactions for YH_2, ScH_2, and NdH_2. Clearly the ScH monohydride, which may be considered as an intermediate state as one proceeds in hydrogenation toward dihydride or trihydride phases, is sensitive to pressure. Note that the hydrogens occupy the tetrahedral sites of a Sc fcc lattice in CaF_2-type ScH_2 and the octahedral interstitial sites in a proposed NaCl-type ScH. Therefore, motion involving these sites is certainly involved in hydrogenation.[9]

While there is recent experimental work on ScH_2 under pressure,[10] it seems to us that much remains to be learned about the structure and interconversions of compressed scandium hydrides. For example, the effect of pressure, via external hydrogen pressurization and inherent compression, on the crystal structures of ScH and ScH_2 is not well understood. In addition, little is known, at P = 1 atm or elevated pressures, about the monohydride, ScH, at any temperature.

We proceed in this paper to a theoretical exploration of the Sc−H phase diagram, within a static approximation. The possible structures of ScH_n (n = 1−3) over a range of pressures up to 500 GPa, with relative compressions reaching $V_0/V \sim 3.0$ (V_0 is the volume of the most stable phase at 1 atm, and V is the volume of the most stable phase at each stable pressure range), are investigated. We examine in detail the evolution of the optimum ground-state static structures of the various hydrides as a function of pressure, as well as their phonon spectra and zero-point energies, and the corresponding electronic band structures of the stable phases predicted. Our aim is to provide a systematic theoretical study of pressure-induced phase transitions in scandium hydrides. The potential existence of higher hydrides of Sc will be the subject of a subsequent study. The computational methodology we have used is fully described in the following section.

THEORETICAL METHODS

We searched for ScH_n (n = 1−3) static ground-state structures using the crystal structure analysis by particle swarm optimization methodology[11] as implemented in the CALYPSO code.[12] This method has been benchmarked on a variety of known systems and has made several successful predictions of high-pressure structures of, for example, Li,[13] Mg,[14] and Bi_2Te_3.[15] Our structure searches with system sizes containing up to 6 formula units (f.u.) per simulation cell were performed at pressures of 0−500 GPa. Each generation contains 30−40 structures (the larger the system, the larger the number of structures). The first generation is produced randomly, and then these structures are optimized. For the next generation, 60% of the structures are generated from the lowest-enthalpy structures provided by the previous generation by particle swarm optimization, the others by random choice. These are then reoptimized, and the previous steps are repeated until convergence. We usually explore 30−50 generations (depending on the size of the system) to achieve a converged structure.

The underlying ab initio structural relaxations were carried out using density functional theory using the Perdew−Burke−Ernzerhof exchange−correlation functional,[16] as implemented in the VASP code.[17] The frozen-core all-electron projector-augmented wave (PAW) method[18] was adopted, with H $1s^1$ (cutoff radius $1.1a_0$; we also tried some of our calculations with shorter cutoff radius $0.8a_0$, which does not change our conclusions materially) and Sc treated as $3s^23p^63d^14s^2$ (cutoff radii $2.5a_0$) outside a 10 electron core. The PAW pseudopotential used for Sc can reproduce reasonably well the Fermi surface for pure Sc (see Figure S1 in the Supporting Information). An energy cutoff of 400 eV and appropriate Monkhorst−Pack[19] k meshes were chosen to ensure that enthalpy calculations were well-converged to better than 1 meV/f.u. Phonons were calculated by using density function perturbation theory (DFPT)[20] as implemented in the PHONOPY code.[21]

Calculations using a hybrid density functional (HSE06)[22] were also carried out for some selected cases. In this method, the exchange−correlation functionals are the mixtures of Fock exchange, PBE exchange, and PBE correlation, i.e.

$$E_{xc}^{HSE} = \alpha \cdot E_x^{HF,SR}(\mu) + (1 - \alpha) \cdot E_x^{PBE,SR}(\mu) + E_x^{PBE,LR}(\mu) + E_c^{PBE}$$

The parameter α is the exchange mixing ratio and is determined by perturbation theory (the recommended value is 0.25).[23] The PBE exchange term is decomposed into two parts, short-range (SR) and long-range (LR), while the correlation part is taken totally from PBE. The parameter μ defines the range separation. The optimum value of μ is approximately 0.2−0.3 $Å^{-1}$, and it is 0.2 $Å^{-1}$ for HSE06. The detailed mathematical derivations and tests of HSE06 functionals are given in the literature.[23]

Throughout this paper we will have occasion to look at Sc−Sc, Sc−H, and H−H separations. We need a calibration for what is a normal distance between the nuclei of these atoms. For Sc−Sc and H−H, these can be obtained from the elemental structures, in particular the most stable ones at every pressure. For H_2 these are structures $P6_3/m$ (0−100 GPa) → $C2/c$ (110−200 GPa) → $Cmca$-12 (250−350 GPa),[24] while for elemental Sc we use the hcp phase to represent the complex high-pressure phases in the range from 1 atm to 350 GPa.[25,26]

Downloaded by CORNELL UNIV on September 8, 2015 | http://pubs.acs.org
Publication Date (Web): February 27, 2015 | doi: 10.1021/jp512538e

DOI: 10.1021/jp512538e
J. Phys. Chem. C 2015, 119, 5614−5625

The relevant internuclear separations are given in the figures in section 3 of the Supporting Information.

For Sc−H, we have only the distances in the known ScH_2 and ScH_3 structures, which we will mention. There are also a number of known molecular compounds of Sc, which also give us an idea of Sc−H separations. For instance, ScH, ScH_2, ScH_3, and $(H_2)ScH_2$ have been observed in matrix isolation experiments,[27,28] with Sc−H separation values calculated as 1.76 Å in ScH[28] (the experimental value is 1.78 Å[29]) and 1.82 Å in ScH_2 and ScH_3. There are also spectroscopic studies of diatomic ScH in molecular beams.[30]

We proceed below to discuss the possible static structures for the three hydrides over the pressure range of 1 atm to 400 GPa. For each stoichiometry, a discussion of harmonic zero-point energies (ZPEs) follows the description of the structures our search reveals.

RESULTS AND DISCUSSION

ScH. Structural searches for the monohydride, ScH, were performed at pressures of 1 atm to 300 GPa. Interestingly, below 15 GPa we find several new structures which are calculated to be more stable enthalpically than the suggested[8] $Fm\bar{3}m$ NaCl-type of ScH (Z = 4, see Figure 3a). The most stable phase we calculate to be the tetragonal $P4_2/mmc$ structure Z = 2, see Figure 3b, in which hydrogen atoms are tetrahedrally coordinated by Sc, with Sc−H separations of 2.05 Å at 1 atm. Other phases are metastable $F\bar{4}3m$ (GaAs type, Z = 4, Figure 3c), $P4/nmm$ (Z = 2, Figure 3d), $Pnma$ (Z = 4, Figure 3e) and $C222$ (Z = 8, Figure 3f) structures; these we obtained by replacing Nb with Sc in the structures found previously for NbH.[31] In all of these structures, except for rock-salt, H appears in interstitial tetrahedral coordination. All are dynamically stable at P = 1 atm; we will discuss the relevant ZPEs and their influence on phase transformations below.

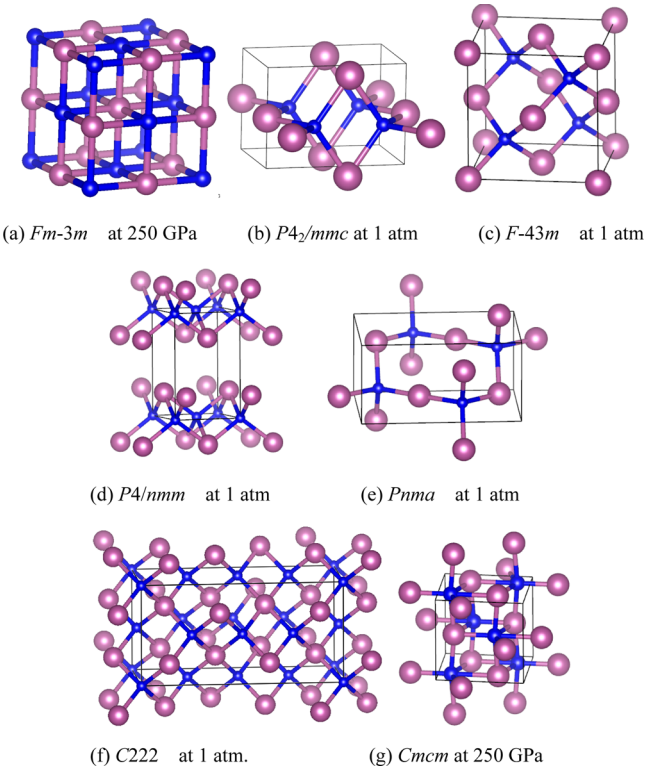

Figure 3. Predicted ground-state static structures of ScH, all but (a) and (g) at 1 atm. The lines indicate Sc−H separations shorter than 2.1 Å.

As a reviewer suggested, the abandonment of the rock-salt structure at P = 1 atm is surprising given that the Pauling radius of Sc^+ is but a little larger than that of Na^+. Shorter and stronger Sc−H contacts are attained in the four-coordinate $P4_2/mmc$ structure, and the crystal orbital Hamiltonian population (COHP) plots, a measure of bond strength (see Supporting Information), indicate some occupation of Sc−H antibonding states just below the Fermi level in the rock-salt structure.

The predicted $P4_2/mmc$ structure at P = 1 atm is so much more stable (~0.25 eV per ScH) in our calculations than the previously proposed[8] rock-salt $Fm\bar{3}m$ structure that we think an experimental search for this alternative phase would be profitable.

Because of the very light mass of the hydrogen atom, quantum effects are expected to be a priori important, and the hydrogen zero-point energy may well be large enough to affect the overall structural stability range of the computed phases.[24] We estimated the ZPEs for each ScH, pure H_2, and Sc under pressure using $E_{ZPE} = 1/2\Sigma_{qj}\hbar\omega_j(q)$ within the harmonic approximation. Here, j indicates a phonon branch at wave vector q and $\omega_j(q)$ is the frequency at wave vector q in the zone and calculated using the PHONOPY code. The results are summarized in Table 1.

Table 1. Calculated Zero-Point Energies, per Atom, for ScH, Sc, and H_2 at 1 atm and Under Pressure

system	space group	pressure (GPa)	zero-point energies (eV/atom)
ScH	$P4_2/mmc$	1 atm	0.118
		10	0.133
	$Pnma$	1 atm	0.117
	$Fm\bar{3}m$	1 atm	0.084
		10	0.102
		50	0.143
		250	0.223
	$Cmcm$	250	0.215
Sc	$P6_3/mmc$	1 atm	0.029
H_2	$P6_3/m$	1 atm	0.129
	$C2/c$	100	0.261
	$Cmca$-12	200	0.282
		300	0.301

Figure 4 shows the detailed enthalpy relations of the various structures in the low-pressure regime. The phases are all (except for rock-salt at lowest pressure) within 0.1 eV per formula unit of each other in enthalpy. This value is actually smaller than the zero-point energies (ZPEs) calculated in the harmonic approximation for the individual structures. The ZPEs are of the order of 0.24 eV per formula at 1 atm and are very similar for all of them (this matter is taken up below). The enthalpy difference between the various structures is also quite close to typical thermal energies. This argues for a self-consistent treatment of the phonons, regrettably not something our resources permit at present.

As the pressure increases in our calculations, the above-mentioned structures are rapidly destabilized relative to the rock-salt $Fm\bar{3}m$ structure (Figure 4), which was also predicted by the structural simulations by us between 20−250 GPa. In the $Fm\bar{3}m$ structure, hydrogen atoms are octahedrally coordinated by Sc (and vice versa) with Sc−H separations of

Downloaded by CORNELL UNIV on September 8, 2015 | http://pubs.acs.org
Publication Date (Web): February 27, 2015 | doi: 10.1021/jp512538e

DOI: 10.1021/jp512538e
J. Phys. Chem. C 2015, 119, 5614−5625

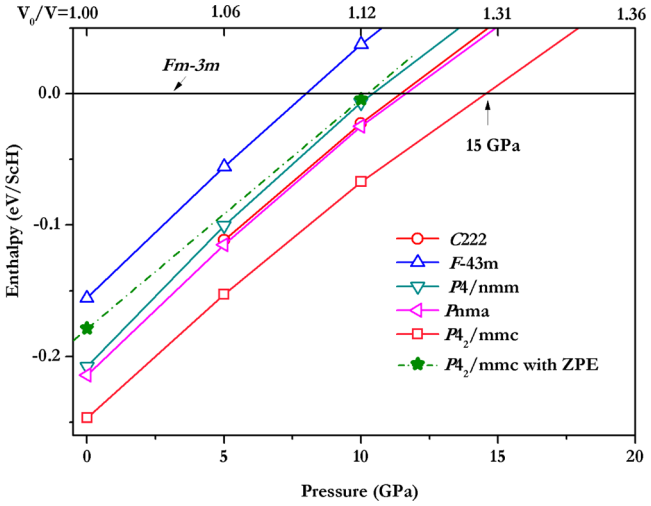

Figure 4. Ground-state static enthalpy curves per formula unit as a function of pressure for ScH, relative to that for the rock-salt $Fm\bar{3}m$ structure in the low-pressure regime. For one structure we move beyond the static approximation, including harmonic ZPEs. The relative compression (V_0/V) is also given for the corresponding pressures (upper horizontal axis).

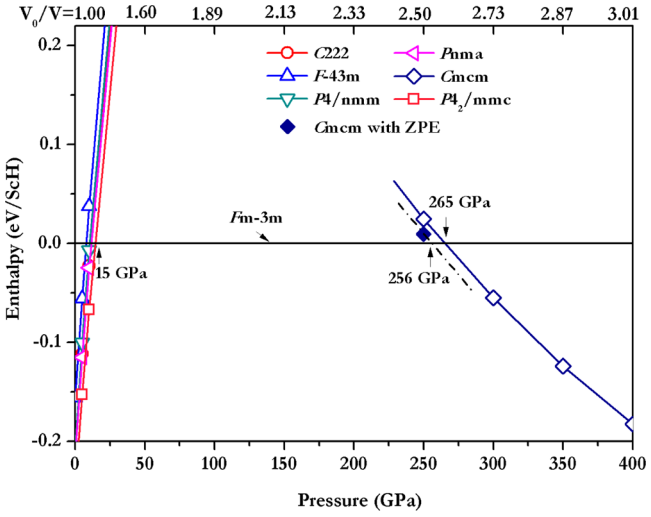

Figure 5. Ground-state enthalpy curves per formula unit as a function of pressure for ScH (static calculations), with respect to that for the rock-salt $Fm\bar{3}m$ structure in the entire pressure range studied. The relative compression (V_0/V) is also given for the corresponding pressures (upper horizontal axis).

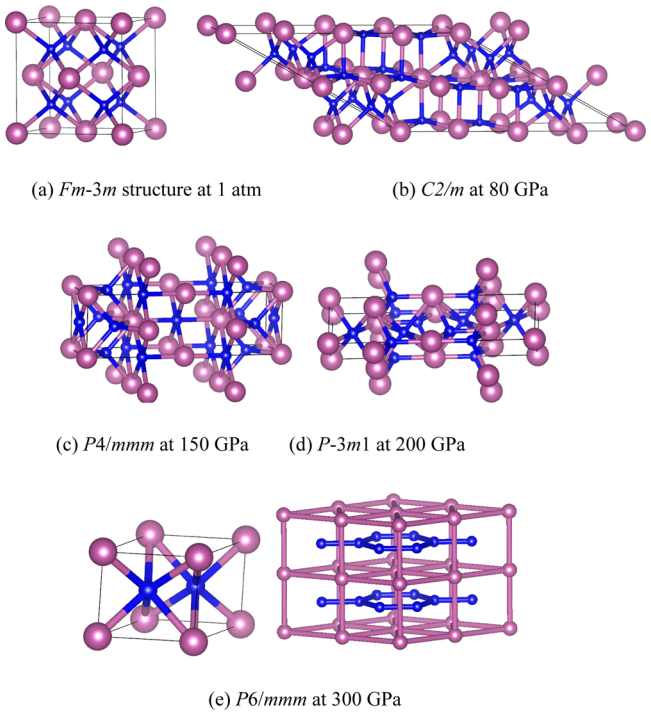

Figure 6. Predicted ground-state static structures of ScH_2 at various pressures.

2.27 Å at 1 atm and 1.74 Å at 250 GPa. If ZPEs are included, the $P4_2/mmc$ phase will become stable at a lower pressure, ~10 GPa, than it would be without consideration of zero-point energies because the $Fm\bar{3}m$ structure has a lower ZPE at the same pressure (e.g., 0.17 eV per formula at 1 atm). The evolution of H coordination in ScH with increasing pressure, from tetrahedral to octahedral, is consistent with previous work[31] and also with the anticipated generalization that the number of neighbors of a hydrogen-occupied site is likely to increase with increasing pressure.[32]

At 300 GPa, a new static structure for ScH emerges in our calculations. This is an orthorhombic *Cmcm* structure (Z = 4, Figure 1g). In this phase, the hydrogen atoms are also octahedrally coordinated by Sc, though the octahedron is distorted with one Sc−H separation of 1.97 Å, 1.77 Å (two), and 1.71 Å (three); the numbers quoted are for 250 GPa. The *Cmcm* structure can be viewed as a distorted rock-salt structure; indeed, there is a relatively flat enthalpy surface between it and perfect rock-salt at 250−300 GPa (see Figure S9 in the Supporting Information). Clearly, calculations including dynamic displacements of hydrogens, and thus approximating the effect of temperature, are needed to delineate structural preferences in this pressure regime.

Above ~265 GPa, the *Cmcm* structure becomes thermodynamically stable relative to the $Fm\bar{3}m$ structure,[33] and the structural preference is pronounced.

We now show the phase enthalpy relationships computed for ScH in a larger pressure window, as in Figure 5. The sequence of phase transitions is $P4_2/mmc \rightarrow Fm\bar{3}m \rightarrow Cmcm$, the transitions calculated to occur at 15 and 265 GPa, respectively. Our predicted ground-state structures for ScH are all enthalpically stable with respect to separation into the elements themselves over the entire pressure range studied. The detailed enthalpy curves are given in Figures S2 and S3 in the Supporting Information.

ScH_2. For the ground-state dihydride, at 1 atm and up to ~75 GPa, we find that the CaF_2 type $Fm\bar{3}m$ structure (Z = 4, Figure 6a) is the most stable enthalpically. This is in good agreement with the experimental results at room temperature,[10,34] though it is clear that our calculations are static, as mentioned earlier, and hence do not include the effect of temperature. The calculated Sc−H separations of 2.07 Å match the experimental values at P = 1 atm.[34]

As the pressure is increased, around 75 GPa, three other structures begin to compete in the phase diagram, as Figure 7 shows. One of these is a monoclinic $C2/m$ structure (Z = 8, Figure 6b). If Sc−H separations less than 2.10 Å are used to define coordination, then in this structure hydrogen atoms are four- (tetrahedrally) and five-coordinated by Sc (see Figure S15 in the Supporting Information). The second is a tetragonal $P4/$

Downloaded by CORNELL UNIV on September 8, 2015 | http://pubs.acs.org
Publication Date (Web): February 27, 2015 | doi: 10.1021/jp512538e

DOI: 10.1021/jp512538e
J. Phys. Chem. C 2015, 119, 5614−5625

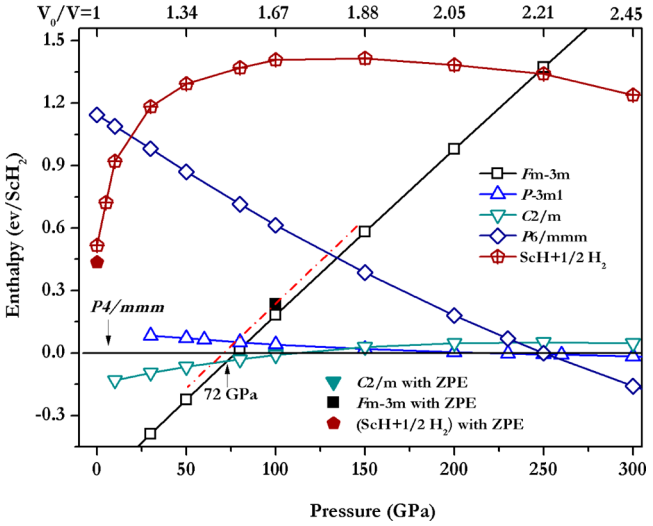

Figure 7. Ground-state static enthalpy curves per formula unit as a function of pressure. In several cases we move beyond the static approximation to show the effect of including harmonic ZPEs. The enthalpy reference is the predicted *P*4/*mmm* structure for static ScH_2 in the entire pressure range studied. The relative enthalpies of ScH + $1/2H_2$ are also presented; for these we took the most stable structures for ScH and H_2 in each pressure range. The relative compression (V_0/V) is indicated at the top.

mmm structure (Figure 6c); its hydrogen atoms are in four-, five-, and six-coordinate Sc environments, the coordination again defined by Sc−H separations less than 2.1 Å (see also Figure S15). Interestingly, we find in this structure some protons that are surrounded by four Sc atoms in a rare approximately square-planar geometry, which has been found in just a few transition-metal complexes at P = 1 atm.[35,36] The third structure competing in this region is a $P\bar{3}m1$ phase (Figure 6d); its protons are tetrahedrally and octahedrally coordinated by Sc.

Between 75 and 225 GPa, the three structures mentioned remain at approximately equal enthalpy, while the fluorite structure is increasingly destabilized. Eventually, above 250 GPa, ScH_2 adopts an MgB_2-type *P*6/*mmm* layer structure (Figure 6e). The protons form a graphene-like honeycomb net (H···H 1.39 Å at 300 GPa) and, judged by Sc−H separations less than 1.78 Å at 300 GPa, are six-coordinated with respect to the Sc ions (see Figure 6e left).

Given the light hydrogens in the structure, vibrational contributions to the relative enthalpy need to be considered, as mentioned earlier. The ZPEs in a harmonic approximation for the various phases are summarized in Table 2 below.

Table 2. Calculated Zero-Point Energies per Atom for Different ScH_2 Structures at 1 atm and Under Pressure

systems	space group	pressure (GPa)	zero-point energies (eV/atom)
ScH_2	*Fm*3*m*	1 atm	0.148
		50	0.199
	*C*2/*m*	80	0.201
	*P*4/*mmm*	150	0.229
		200	0.246
	$P\bar{3}m1$	200	0.243
		250	0.256
	*P*6/*mmm*	250	0.241

We show the phase enthalpy relationships in the entire pressure range studied in Figure 7. The $P\bar{3}m1$ and *P*6/*mmm* structures were also predicted in NbH_2[31] and CaH_2[37] at high pressures, respectively. Also in Figure 7 are the enthalpies of decomposition of ScH_2 to ScH + H_2; these indicate that the ground state of ScH_2 is enthalpically stable with respect to decomposition at 1 atm and also under pressure. This conclusion is in agreement with the experimental result that it is hard to detect ScH during the reaction of Sc and H_2 at 1 atm.[38]

Between 200−260 GPa, the $P\bar{3}m1$, *P*4/*mmm*, and *P*6/*mmm* structures are very close to each other in enthalpy, in fact within 0.01 eV per formula unit. This value is also smaller than the ZPEs for the individual structures, which are of the order of 0.72 eV per formula and are similar for all of them. As Figure S13 in the Supporting Information shows, after inclusion of ZPE (by simple addition, a less than satisfactory approximation), $P\bar{3}m1$ becomes more stable than *P*4/*mmm* at 200 GPa, while *P*6/*mmm* is stabilized over $P\bar{3}m1$ at 250 GPa.

ScH_3. Our structural searches between 1 atm and 500 GPa predict that the ground-state static phase transition sequence of the trihydride is $P6_3$ (Z = 6, Figure 8a) → $Fm\bar{3}m$ (Z = 4, Figure 8d) → $P6_3/mmc$ (YH_3-type,[6] Z = 2, Figure 8g) → *Cmcm* (Z = 4, Figure 8h); the corresponding transition pressures are 29, 360, and 483 GPa, respectively. As will become clear in the discussion below, in some pressure ranges several structures compete enthalpically. The general result is in good agreement with the recent theoretical calculations of Kong et al.,[39] who used the known high-pressure structures of YH_3, but replacing Y by Sc. One thing that should be mentioned is that the $P6_3$ structure of ScH_3 we found is more stable than the $P6_3/mmc$ (GdH_3 type) structure reported by Kong et al. (see Supporting Information).

Of every three hydrogen atoms in the GdH_3-type ScH_3, two are found close to the tetrahedral sites; we shall denote these atoms by H(T). The third hydrogen atom, which we shall denote H(M), is located in, or close to, the heavy atom plane. Similar to the case of YH_3,[5] the predicted low-pressure $P6_3$ structure can be obtained from the GdH_3 structure by tripling it in the basal *ab* plane, such that there are three hydrogen atoms in each metal plane. The tripled hexagonal unit cell contains 24 atoms with a stoichiometry Sc_6H_{18}. All the H(M) atoms move out of the metal plane, one-third of them by about 0.06 *c*, one-third by about −0.06 *c*, and the rest by about 0.01 *c*. Comparing this resulting structure to the GdH_3-type we observe that there is a screw axis through the H(M) atoms that are displaced by −0.06 *c*. The H(T) atoms are also slightly displaced as compared to their positions in the GdH_3 structure. This is a reasonable approximation of the supposed experimental structure of $ScH_{2.9}$, in which the protons atoms randomly occupy one of the two equivalent positions in the Sc atom basal plane (Figure 8c). In Figure 9 we show the calculated and observed powder diffraction patterns for our new structural suggestion, and the agreement is excellent. We are unable to model the $ScH_{2.9}$ nonstoichiometry in detail.

The zero-point energies of the various ScH_3 structures, potentially significant in phase relationships, are summarized in Table 3.

Interestingly, even at 1 atm, ScH_3 is still stable relative to decomposition into ScH_2 and H_2, as seen in Figure 10, which shows the enthalpy relations of the various structures in the low-pressure regime. However, the enthalpy difference is not large, about 0.14 eV per formula unit at 1 atm, not including

Downloaded by CORNELL UNIV on September 8, 2015 | http://pubs.acs.org
Publication Date (Web): February 27, 2015 | doi: 10.1021/jp512538e

DOI: 10.1021/jp512538e
J. Phys. Chem. C 2015, 119, 5614−5625

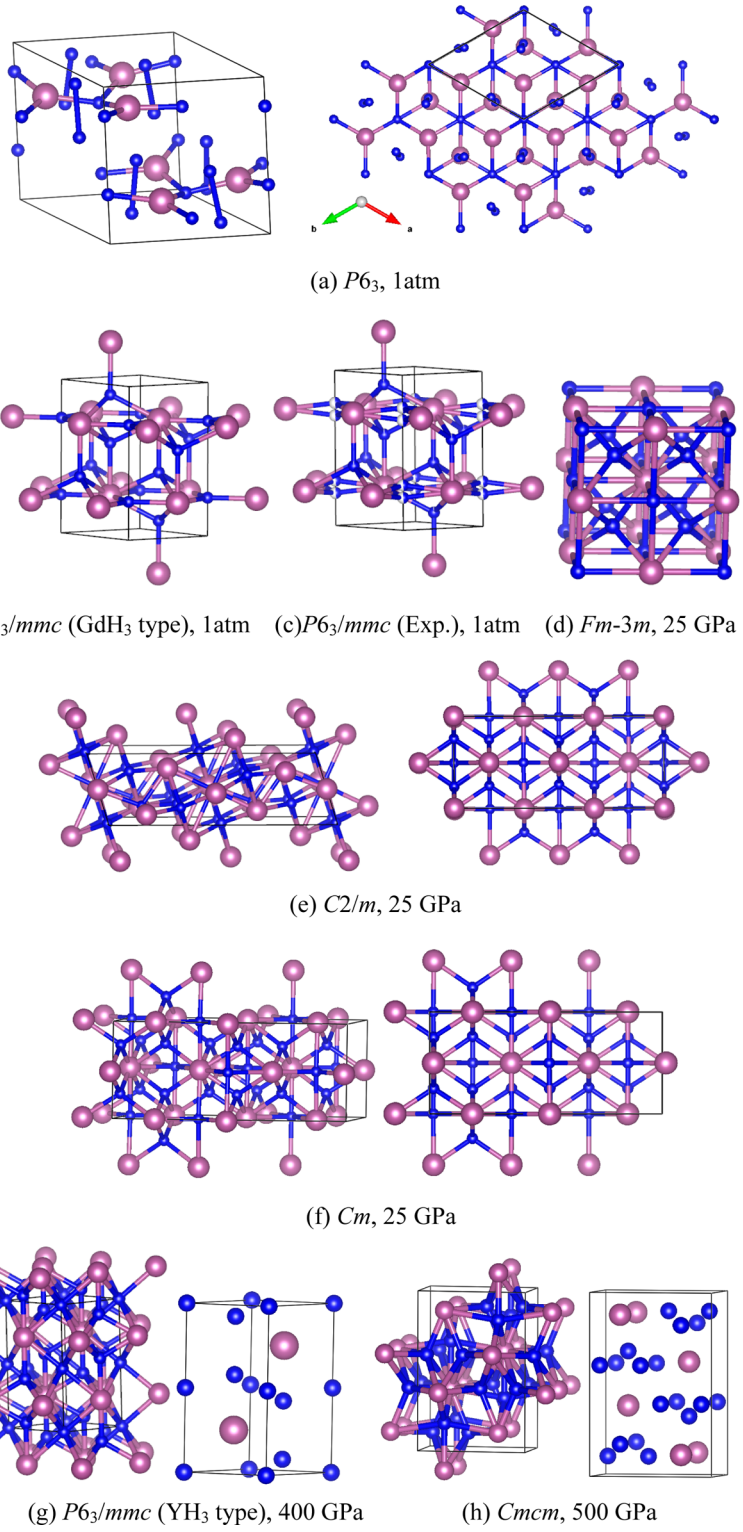

Figure 8. Predicted static ground-state high-pressure $P6_3$, $C2/m$, $Fm\bar{3}m$, $P6_3/mmc$(YH_3 type), and $Cmcm$ structures of ScH_3 (purple, Sc; blue, H). Panel b is the reported structure of ScH_3 at 1 atm,[39] while panel c is the supposed experimental structure. In panel c, note the half-occupied sites are marked by half-blue, half-white spheres.

ZPEs, but 0.10 eV when including ZPEs. As a reviewer has pointed out, considering that the entropy term in the free energy for H_2 at 300 K equals 0.2 eV,[4] it is evident that ScH_3 loses some H_2 and becomes H-deficient, nonstoichiometric. Actually, $ScH_{2.9}$ can be stored in liquid nitrogen and was experimentally observed to decompose to ScH_2 + H_2 at elevated temperatures at 1 atm.[1]

In our calculations, above 29 GPa the $P6_3$ structure of the trihydride is no longer the most stable choice. Three structures of approximately equal enthalpy compete at this approximate pressure: the $P6_3$ (Z = 6) structure we predict, $Fm\bar{3}m$ (Z = 4),

Downloaded by CORNELL UNIV on September 8, 2015 | http://pubs.acs.org
Publication Date (Web): February 27, 2015 | doi: 10.1021/jp512538e

DOI: 10.1021/jp512538e
J. Phys. Chem. C 2015, 119, 5614−5625

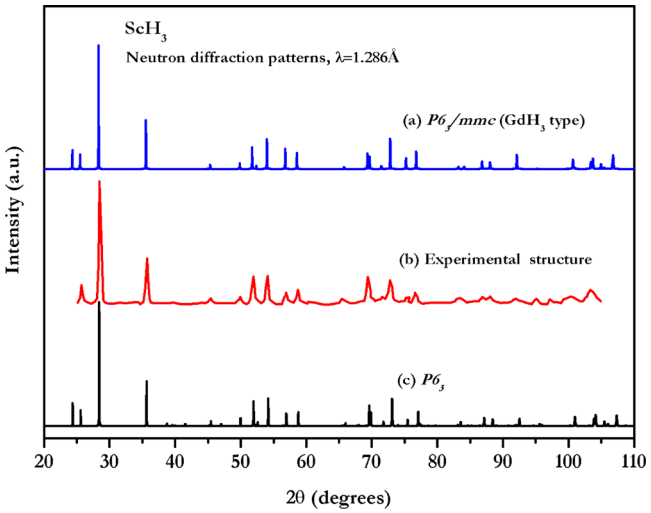

Figure 9. Neutron diffraction patterns of the structure of ScH_3 at standard conditions: (a) calculated powder diffraction pattern of the $P6_3/mmc$ (GdH_3-type) structure, (b) the experimental diffraction pattern, and (c) the calculated powder diffraction pattern of the $P6_3$ structure.

Table 3. Calculated Zero-Point Energies per Atom for ScH_3 at 1 atm and Under Pressure

systems	space group	pressure (GPa)	zero-point energies (eV/atom)
ScH_3	$P6_3$	1 atm	0.153
	$C2/m$	25	0.175
	$Fm\bar{3}m$	25	0.168
		50	0.191
		350	0.301
	$P6_3/mmc$ (YH_3 type)	400	0.310
	$Cmcm$	550	0.322

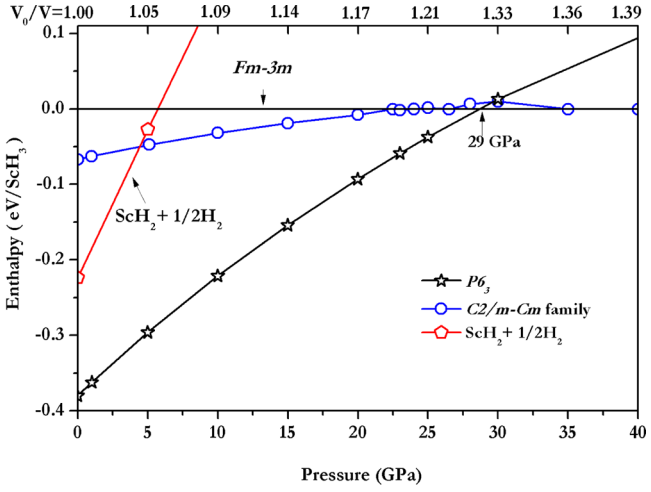

Figure 10. Ground-state static enthalpy curves per formula unit as a function of pressure (with respect to the $Fm\bar{3}m$ structure) for static ScH_3 in the low-pressure regime. The relative enthalpies of $ScH_2 + H_2$ are also shown; here we used the most stable structures for ScH_2 and H_2 in each pressure range.

and a family of structures that is $C2/m$ ($Z = 6$) or Cm ($Z = 6$). The enthalpic similarity of the three structures reflects an underlying structural similarity that merits further discussion.[7,40]

In the $Fm\bar{3}m$ structure, protons occupy all the T and O sites of an fcc lattice with Sc−H separation of 1.95 and 2.25 Å at 25 GPa, respectively (Figure 8d). The $C2/m$ structure was suggested as a periodically distorted form of the fcc structure (a possible Peierls distortion), thought to be a candidate model for the intermediate phase.[40] In this structure, H atoms are also tetrahedrally and octahedrally coordinated by Sc, but now unsymmetrically, with Sc−H separations of 1.96 and 1.97 Å in the tetrahedron and 2.13, 2.22, and 2.46 Å in the octahedron at 25 GPa (Figure 8e).

For the transition from the hcp to the fcc heavy atom lattice in ScH_3, it was suggested that the pathway conserves the hcp basal planes and also the $(110)_h$ planes,[2] but in such a way that the ABABAB sequence of the hcp form is altered to the ABCABC sequence of the fcc form. After the phase transition, the $(110)_h$ planes become the equivalent $(220)_f$ planes in the fcc phase.[2] The movement of the atoms, both Sc and H, during the hcp-to-fcc transition can be separated conceptually into six sliding steps, throughout which Cm symmetry is maintained.[41] The assumption here is that this is also the symmetry of the intermediate phase(s) in ScH_3.

More recently, Pakornchote et al.[7] investigated the hcp-to-fcc transformation path of ScH_3 under high pressure, proposing that the intermediate phase was of Cm ($Z = 6$) symmetry. As Figure 8e,f shows, the $C2/m$ and Cm structures suggested are very similar. Depending on the tolerance used in automated symmetry assignment (CASTEP[42] with tolerance larger than 0.01), the program assigns to the structure either Cm or $C2/m$ symmetry. Recognizing how close to each other these structures are, we will refer to them as a single $C2/m$-Cm family. Above 30 GPa, the $C2/m$ structure transforms to the $Fm\bar{3}m$ structure during the VASP optimization process. To obtain a reliable picture of phase stabilities in this region, accurate dynamic calculations beyond our means will be needed.

Figure 11 shows enthalpy relations of the various structures in the entire pressure regime studied, a 10-fold greater pressure

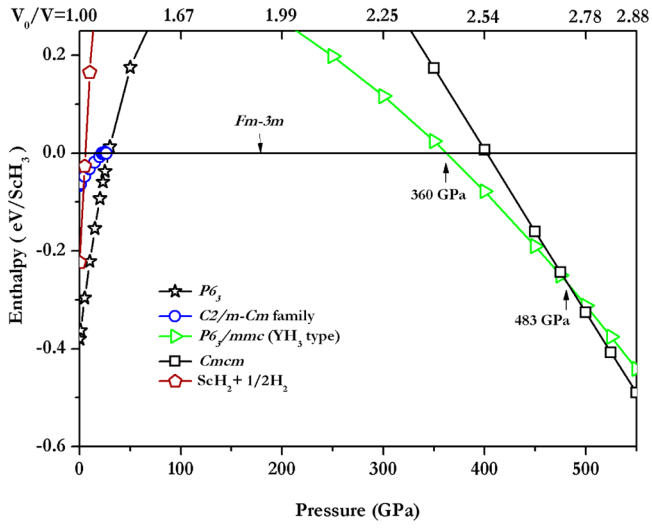

Figure 11. Ground-state static enthalpy curves per formula unit as a function of pressure with respect to the predicted $Fm\bar{3}m$ structure for static ScH_3 in the entire pressure range studied. The relative compression (V_0/V) is indicated on upper horizontal axis.

Downloaded by CORNELL UNIV on September 8, 2015 | http://pubs.acs.org
Publication Date (Web): February 27, 2015 | doi: 10.1021/jp512538e

DOI: 10.1021/jp512538e
J. Phys. Chem. C 2015, 119, 5614−5625

range than that of Figure 10. The $Fm\bar{3}m$ structure has a wide range of stability between 30−360 GPa. Above 360 GPa, it is finally overtaken by a $P6_3/mmc$ structure (YH_3 type, $Z = 2$) in which H atoms are also tetrahedrally and octahedrally coordinated by Sc (Figure 8g). Above 483 GPa, a still more stable structure enters, an orthorhombic $Cmcm$ structure ($Z = 4$), in which H atoms are 5-fold coordinated (Figure 8h). The shortest separation of two H atoms in the $Cmcm$ structure is 1.20 Å at 500 GPa ($V_0/V = 2.78$), which is longer than the shortest separation of 0.85−0.88 Å in pure solid hydrogen (monatomic) at the same pressure[43] (see also Figure S4 in the Supporting Information). It appears that there are no semimolecular paired hydrogens in the high-pressure structure of ScH_3.[44]

Dynamical Stability for Different Stoichiometries. We have also studied the dynamical stability of the predicted ScH_n ($n = 1-3$) structures by calculating their phonon dispersion curves. We find that all of the predicted structures of each hydride are dynamically stable (see Figures S6, S12, and S17 in the Supporting Information). The calculated phonon frequencies of different structures in scandium hydrides separate naturally into two groups: low-frequency modes (mostly associated with Sc motions) and high-frequency modes, those dominated by light H atoms. The gap between the low- and high-frequency modes gradually decreases as the content of hydrogen increases, and as expected, the highest frequencies also increase with increasing pressure.

The calculated ZPEs for the various structures have been given in Tables 1−3.

Let us discuss now in more detail the structure for ScH_3. The symmetric $P6_3/mmc$ structure formerly suggested,[39] shown in Figure 8b, is not dynamically stable from 1 atm to 25 GPa (see Figure S17 in the Supporting Information). We will get the $P6_3$ structure when we follow the phonon of imaginary frequency to a more stable minimum. The $P6_3$ structure is dynamically stable and, as expected, is more stable than the $P6_3/mmc$ structure (see also Figure S16 in the Supporting Information). Recall that the experimentally observed lower-symmetry structure is for a nonstoichiometric $ScH_{2.9}$ phase. The fractional occupation is consistent with motion away from a more symmetrical structure, but the details remain to be worked out.

Two Disproportionations. With the phase transition sequences of ScH, ScH_2, and ScH_3 in hand, we can approach the pressure dependence of the ScH_2 disproportionation reaction. Figure 12 compares the enthalpy of the reaction

$$ScH_2 \rightarrow \frac{1}{2}ScH + \frac{1}{2}ScH_3$$

with and without ZPEs. Positive enthalpies mark a region of stability of ScH_2, negative ones of ScH + ScH_3.

Figure 12 shows that ScH_2 is enthalpically stable below 80 GPa but becomes unstable compared to ScH and ScH_3 at higher pressure. This is in agreement with the experimental observations,[9] though the transition pressure was not given in the work cited. To obtain a calibration, we also computed with similar methodology the relative formation enthalpy of LaH_2 disproportionation to LaH and LaH_3. The results, shown in Figure S18 in the Supporting Information, give a transition pressure for LaH_2 of 10 GPa, which is in good agreement with both experimental and theoretical results.[9]

At 80 GPa, ScH_2 adopts the $C2/m$ structure while ScH and ScH_3 have the fcc structures at this pressure. This implies that the rock-salt-type monohydride (ScH) may be formed by the pressure-induced disproportionation of rock-salt-like $C2/m$ ScH_2, not fcc ScH_2. This is a little different from the case of LaH_2, in which LaH_2 adopts the fcc structure near the transition pressure.

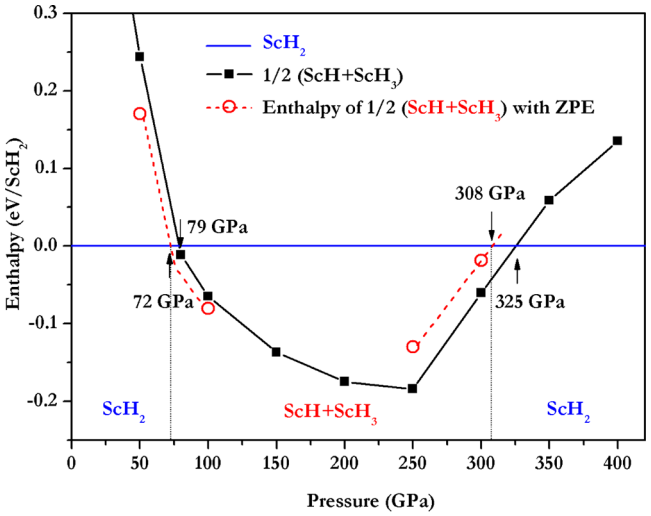

Figure 12. Static ground-state enthalpy curves per formula unit (black curves) as a function of pressure with respect to ScH_2. We also move beyond the static approximation by estimating the contribution of ZPEs (red dashed lines). We have considered the most stable structures for ScH, ScH_2, and ScH_3 found in this work at the specified pressure ranges. The ZPE differences are taken to be approximately pressure-independent. The vertical dotted lines separate the different stable regions.

Most interesting is a prediction that our studies make at higher pressure: we find, as Figure 12 shows, that ScH_2 is stabilized again around 325 GPa, now in a pressure-induced comproportionation reaction of ScH and ScH_3. When ZPEs are included, both the disproportionation and comproportionation reactions may occur at a somewhat lower pressure, ∼72 GPa and ∼308 GPa, respectively. This prediction remains to be tested experimentally.

The effects of ZPE on ground-state phase transition

$$ScH_2 \rightarrow \frac{1}{2}ScH + \frac{1}{2}ScH_3$$

are best shown graphically, which is also done in Figure 12. The assumption is made that the total enthalpy is the sum of that of the static system and the contribution of the phonons determined in a harmonic approximation (eventually a self-consistent approach to this may be required). ScH_2 has a larger ZPE of 0.597 eV per formula unit at 50 GPa when compared with the corresponding sum of ZPEs for ScH_3 and ScH at 50 GPa [0.525 eV/(ScH_3+ScH)/2], indicating that after inclusion of ZPE, ScH_3 + ScH may become stable at a slightly lower pressure, ∼ 72 GPa (see Figure 12).

If no ScH is present, ScH_3 is enthalpically stable in the studied pressure range of 0−500 GPa. This is especially true for the fcc-ScH_3 structure, which has a wide range of stability between 30−360 GPa. We doubt whether any higher hydrides exist in this pressure range. However, the consistency of the geometries we find for ScH, ScH_2, and ScH_3, and the good agreement of the enthalpies of the disproportionation reaction of ScH_2 with experimental results, encourages us to examine other, higher hydrides. These will be discussed in detail in a further paper.

Downloaded by CORNELL UNIV on September 8, 2015 | http://pubs.acs.org
Publication Date (Web): February 27, 2015 | doi: 10.1021/jp512538e

DOI: 10.1021/jp512538e
J. Phys. Chem. C 2015, 119, 5614−5625

We now turn to the other disproportionation, that of monohydride. Figure 13 shows the enthalpy of ScH relative to

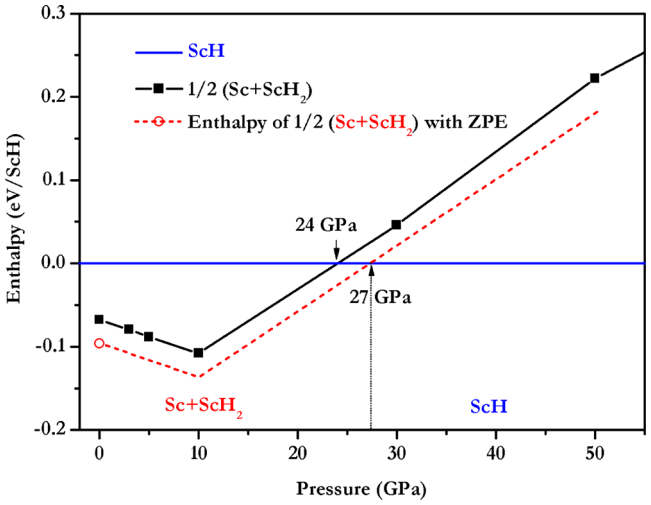

Figure 13. Ground-state enthalpy curves per formula unit as a function of pressure with respect to ScH. We have considered the most stable structures for ScH and ScH_2 at each stable pressure range and the $P6_3/mmc$ structure for Sc. The ZPE differences are taken to be approximately pressure-independent.

$1/2(ScH_2 + Sc)$. Interestingly, we find pure ScH can be also obtained by squeezing ScH_2 and Sc around 24 GPa. When ZPEs are added, ScH is stabilized at a greater pressure, around 27 GPa, because ScH has a larger ZPE than the corresponding sum of ScH_2 and Sc ZPEs.

Theoretical Scandium–Hydrogen Phase Diagram. Let us now assemble the enthalpy relationships for the ScH_n (n = 1, 2, 3) series in the form of a convex hull of comparative stability (see Figure 14). The reference levels are scandium and pure

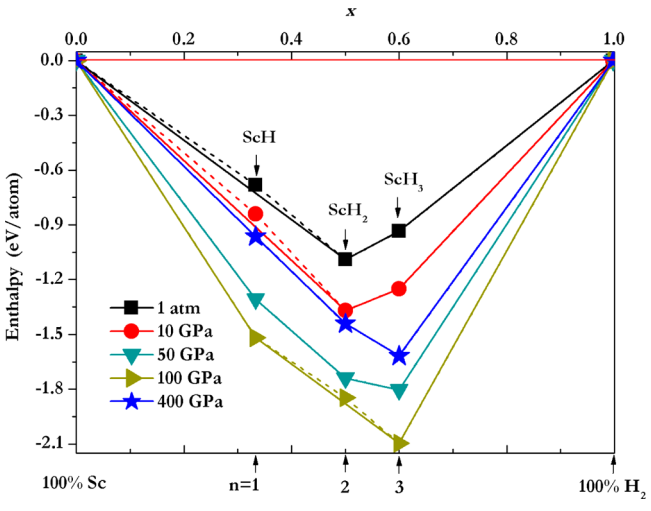

Figure 14. Ground-state static enthalpy of formation per atom of the ScH_n (n = 1, 2, 3) phases with respect to their separated counterparts; hydrogen molar content (x = 0 corresponds to pure scandium, x = 1 to pure hydrogen) for the ground state and P = 1 atm, 10, 50, 100, and 400 GPa. The stoichiometric index n (in ScH_n) is indicated at the bottom. The symbols on the solid line indicate that the hydride is stable at the corresponding pressure, while those on the dashed line are metastable, unstable with respect to decomposition or disproportionation into other hydrides or hydrogen.

hydrogen, each in its most stable form at the pressure specified (there is an approximation for Sc as mentioned before). More information on stability at other pressures (30, 80, and 250 GPa) is given in the Supporting Information (Figure S22).

As can be seen in Figure 14, from the lowest pressures, ScH, ScH_2, and ScH_3 are very stable with respect to decomposition into the elements. Indeed, all are known experimentally. ScH_2 is the global thermodynamic minimum between 1 atm and 50 GPa. Interestingly, in this pressure range, ScH can be obtained by the compression of a mixture of ScH_2 and Sc (see also Figure 13), while ScH_3 can be obtained by the compression of a mixture of ScH_2 and H_2. Both ScH and ScH_3 can actually be obtained simultaneously if ScH_2 is compressed up to 80 GPa. These results are in agreement with the experimental observations.

Above 80 GPa, ScH_3 achieves a global thermodynamic minimum. As we saw in Figure 12, at still higher pressures, ScH_2 regains stability and can be obtained again by the compression of a mixture of ScH and ScH_3 to 325 GPa.

Electronic Structure of the Scandium Hydrides. The band structures and total densities of states (DOS) of ScH, ScH_2, and ScH_3, all at P = 1 atm, are displayed in Figures 15,

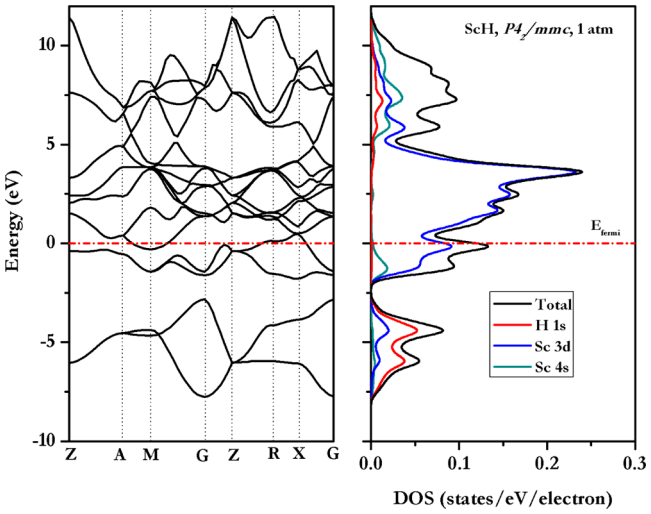

Figure 15. Electronic band structure and DOS for the $P4_2/mmc$ structure of ScH at 1 atm.

16, and 17, respectively, along with the projected DOS of Sc 3d and 4s and H 1s. Assuming that hydrogen becomes hydridic (tending toward H^-) in its interaction with scandium, one would expect metallic ScH and ScH_2 and semiconducting ScH_3.

The general expectation is met. The calculated gap is 0.8 eV for ScH_3, while the observed optical gap is 1.7 eV.[40] An improvement is likely if we move in our treatment of correlation beyond LDA band-structure calculations (as was observed for YH_3,[45] which experimentally has a gap of 2.6 eV, but comes out metallic in LDA calculations). HSE06 calculations were initiated for this purpose, and it was found that the band gap of ScH_3 calculated by HSE06 method is 1.5 eV, which is in reasonable agreement with the experimental value (see Figure S19 in the Supporting Information).

Let us discuss these densities of states in a little more detail. First, the H electron density of states is concentrated into a peak around −6 eV that is spread out broadly but remains mainly below the Fermi level. If the hydrogen states were fully occupied with two electrons per H, we would have entirely

Downloaded by CORNELL UNIV on September 8, 2015 | http://pubs.acs.org
Publication Date (Web): February 27, 2015 | doi: 10.1021/jp512538e

DOI: 10.1021/jp512538e
J. Phys. Chem. C 2015, 119, 5614−5625

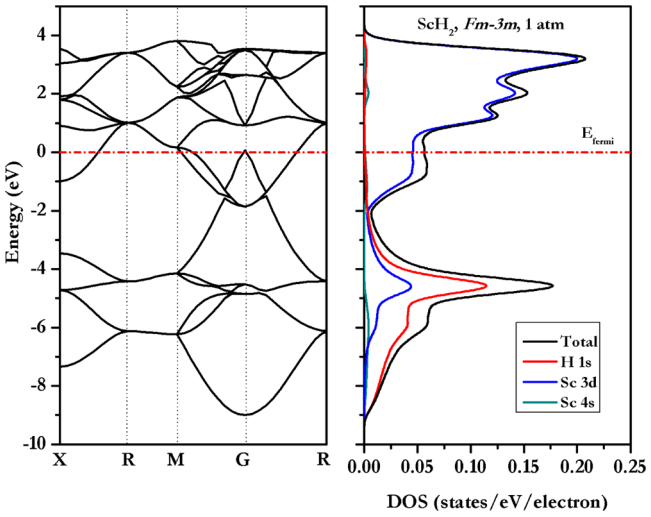

Figure 16. Electronic band structure and DOS for the $Fm\bar{3}m$ structure of ScH_2 at 1 atm.

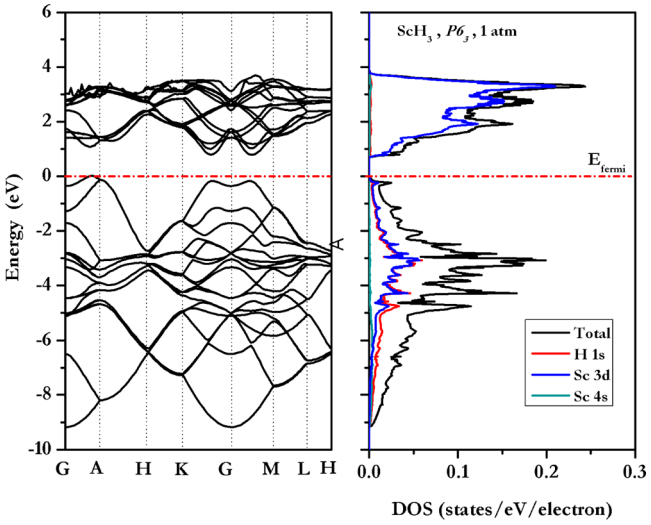

Figure 17. Electronic band structures and DOS for the $P6_3$ structure of ScH_3 at 1 atm.

hydridic hydrogens. But there clearly is some interaction between Sc 3d states and the hydride 1s. This is found in energy regions where there is density in both Sc and H states, from −8 to −3 eV, indicating their likely mixing. The covalence we see (also probed in the Supporting Information, section 9, Figures S25−S27, through an analysis of crystal orbital Hamiltonian populations) is in qualitative agreement with the conclusions drawn from the studies of ScH_2 both experimentally[46] and theoretically.[47]

In the Supporting Information, the reader will find two further sections. The first discusses in detail the interatomic separations and coordination numbers as n varies in ScH_n. The Sc−Sc separation actually expands in response to hydrogen insertion, relative to the pure element, in this pressure range. The Sc−H separations decrease with pressure, and as expected, the Sc coordination in H increases.

In a second section we relate a comparison of scandium hydrides to the hydrides of Y and La, which are below Sc in the periodic table, and of Ca, to the left of Sc. There are many similarities in Y and La hydride chemistry, but there are few for Ca, except for CaH_2.

CONCLUSIONS

The scandium hydride system is certainly rich in structural possibilities, as we have seen. All three compositions, ScH, ScH_2, and ScH_3, go through a range of structures as the pressure is raised, in which the coordination of the Sc in hydrogens increases, while the Sc−Sc separations remain relatively constant. Most interesting among the individual structures is our prediction of several stable P = 1 atm ScH phases which are calculated to be a lower enthalpy than the previously suggested rock-salt structure. We also point to a possible modification of the assigned P = 1 atm ScH_3 structure. In their electronic structures one sees the hydridic nature of the H in these compounds. ScH and ScH_2 are definitely metallic and remain so as the pressure is elevated. ScH_3 is, as expected, semiconducting.

Equilibria with H_2 are the most direct fact of life for these materials, important to their synthesis as well as to their potential for hydrogen storage. All the hydrides have negative heats of formation from the elements throughout the pressure range studied (1 atm to 400 GPa). Remarkably, ScH_2 is stable with respect to disproportionation to ScH and ScH_3 at both low and high pressures; in the range of ∼75−310 GPa it should spontaneously decompose to ScH and ScH_3. In addition, ScH should be stable with respect to disproportionation to Sc and ScH_2 only above ∼25 GPa. As expected, ScH and ScH_2 are found in our calculations to be metallic at P = 1 atm, and ScH_3 is foudn to be semiconducting. At higher pressures, all there hydrides metallize.

ASSOCIATED CONTENT

Supporting Information

1. Fermi surface of Sc. 2. Enthalpies of ScH with respect to Sc and H_2 as a function of pressure. 3. Sc−Sc separations in Sc and H−H separations in H_2 as a function of pressure. 4. ScH: phonon band structures; electronic band structures and DOS; structural parameters; Sc−Sc and Sc−H separations. 5. ScH_2: phonon band structures; high-pressure enthalpy relationships; electronic band structures and DOS; structural parameters; Sc−Sc and Sc−H separations. 6. ScH_3: enthalpy relationships at low pressure; phonon band structures; electronic band structures and DOS; structural parameters; Sc−Sc and Sc−H separations. 7. Disproportionation reaction of LaH_2 and enthalpy relationships between scandium hydrides. 8. Comparison of electronic band structures and DOS for ScH, ScH_2, and ScH_3 near the phase separation pressure of ScH_2. 9. A crystal orbital Hamiltonian population analysis of bonding in scandium hydrides. 10. Comparison of Sc−Sc and Sc−H separations in scandium hydrides. 11. Interatomic separations and coordination number as n varies in ScH_n. 12. A comparison with neighboring elements. 13. An analysis of the enthalpy of scandium hydride structures based on recently synthesized iron hydrides. This material is available free of charge via the Internet at http://pubs.acs.org.

AUTHOR INFORMATION

Corresponding Author

*E-mail: rh34@cornell.edu.

Notes

The authors declare no competing financial interest.

Downloaded by CORNELL UNIV on September 8, 2015 | http://pubs.acs.org
Publication Date (Web): February 27, 2015 | doi: 10.1021/jp512538e

DOI: 10.1021/jp512538e
J. Phys. Chem. C 2015, 119, 5614−5625

Downloaded by CORNELL UNIV on September 8, 2015 | http://pubs.acs.org
Publication Date (Web): February 27, 2015 | doi: 10.1021/jp512538e

■ ACKNOWLEDGMENTS

We are grateful to Andreas Hermann, Wojciech Grochala, Yanming Ma, D. L. V. K. Prasad, and Huayung Geng for their discussions and to a reviewer for useful comments. We acknowledge support by the National Science Foundation, through research Grants CHE-0910623, CHE-1305872, and DMR-0907425, and EFree, an Energy Frontier Research Center funded by the U.S. Department of Energy (Award DESC0001057 at Cornell). The project was also supported by the National Natural Science Foundation of China (21401173, 21371160, 11305147).

■ REFERENCES

(1) Antonov, V. E.; Bashkin, I. O.; Fedotov, V. K.; Khasanov, S. S.; Hansen, T.; Ivanov, A. S.; Kolesnikov, A. I.; Natkaniec, I. Crystal Structure and Lattice Dynamics of High-Pressure Scandium Trihydride. *Phys. Rev. B: Condens. Matter Mater. Phys.* **2006**, *73*, 054107.

(2) Ohmura, A.; Machida, A.; Watanuki, T.; Aoki, K.; Nakano, S.; Takemura, K. Pressure-Induced Structural Change from Hexagonal to fcc Metal Lattice in Scandium Trihydride. *J. Alloys Compd.* **2007**, *446*−*447*, 598−602.

(3) Ye, X. Q.; Tang, T.; Ao, B. Y.; Luo, D. L.; Sang, G.; Zhu, H. Z. Thermodynamics of Sc-H and Sc-D Systems: Experimental and Theoretical Studies. *J. Fusion Energy* **2013**, *32*, 254−257.

(4) For an excellent overview of metal hydrides, see Grochala, W.; Edwards, P. P. Thermal Decomposition of the Non-Interstitial Hydrides for the Storage and Production of Hydrogen. *Chem. Rev. (Washington, DC, U.S.)* **2004**, *104*, 1283−1316.

(5) van Gelderen, P.; Kelly, P. J.; Brocks, G. Structural and Dynamical Properties of YH_3. *Phys. Rev. B: Condens. Matter Mater. Phys.* **2003**, *68*, 094302.

(6) Yao, Y. S.; Klug, D. D. Consecutive Peierls Distortions and High-Pressure Phase Transitions in YH_3. *Phys. Rev. B: Condens. Matter Mater. Phys.* **2010**, *81*, 140104.

(7) Pakornchote, T.; Pinsook, U.; Bovornratanaraks, T. The hcp to fcc Transformation Path of Scandium Trihydride under High Pressure. *J. Phys.: Condens. Matter* **2014**, *26*, 025405.

(8) Machida, A.; Honda, M.; Hattori, T.; Sano-Furukawa, A.; Watanuki, T.; Katayama, Y.; Aoki, K.; Komatsu, K.; Arima, H.; Ohshita, H.; et al. Formation of NaCl-Type Monodeuteride LaD by the Disproportionation Reaction of LaD_2. *Phys. Rev. Lett.* **2012**, *108*, 205501.

(9) Machida, A.; Watanuki, T.; Kawana, D.; Aoki, K. Phase Separation of Lanthanum Hydride under High Pressure. *Phys. Rev. B: Condens. Matter Mater. Phys.* **2011**, *83*, 054103.

(10) Lityagina, L. M.; Dyuzheva, T. I. Isothermal Compression Study of 3d and 4d Transition Metal Dihydrides I: Compression of ScH_2 up to 27 GPa. *J. Alloys Compd.* **1992**, *179*, 69−71.

(11) Wang, Y. C.; Lv, J.; Zhu, L.; Ma, Y. M. Crystal Structure Prediction via Particle-Swarm Optimization. *Phys. Rev. B: Condens. Matter Mater. Phys.* **2010**, *82*, 094116.

(12) Wang, Y. C.; Lv, J.; Zhu, L.; Ma, Y. M. CALYPSO: A Method for Crystal Structure Prediction. *Comput. Phys. Commun.* **2012**, *183*, 2063−2070.

(13) Lv, J.; Wang, Y. C.; Zhu, L.; Ma, Y. M. Predicted Novel High-Pressure Phases of Lithium. *Phys. Rev. Lett.* **2011**, *106*, 015503.

(14) Li, P. F.; Gao, G. Y.; Wang, Y. C.; Ma, Y. M. Crystal Structures and Exotic Behavior of Magnesium under Pressure. *J. Phys. Chem. C* **2010**, *114*, 21745−21749.

(15) Zhu, L.; Wang, H.; Wang, Y. C.; Lv, J.; Ma, Y.; Cui, Q.; Ma, Y. M.; Zou, G. Substitutional Alloy of Bi and Te at High Pressure. *Phys. Rev. Lett.* **2011**, *106*, 145501.

(16) Perdew, J. P.; Burke, K.; Ernzerhof, M. Generalized Gradient Approximation Made Simple. *Phys. Rev. Lett.* **1996**, *77* (18), 3865−3868.

(17) Kresse, G.; Furthmüller, J. Efficient Iterative Schemes for ab initio Total-Energy Calculations Using a Plane-Wave Basis Set. *Phys. Rev. B: Condens. Matter Mater. Phys.* **1996**, *54*, 11169−11186.

(18) Blöchl, P. E. Projector Augmented-Wave Method. *Phys. Rev. B: Condens. Matter Mater. Phys.* **1994**, *50*, 17953−17979.

(19) Monkhorst, H. J.; Pack, J. D. Special Points for Brillouin-Zone Integrations. *Phys. Rev. B: Solid State* **1976**, *13*, 5188−5192.

(20) Gonze, X.; Lee, C. Dynamical Matrices, Born Effective Charges, Dielectric Permittivity Tensors, and Interatomic Force Constants from Density-Functional Perturbation Theory. *Phys. Rev. B: Condens. Matter Mater. Phys.* **1997**, *55*, 10355−10368.

(21) Togo, A.; Oba, F.; Tanaka, I. First-Principles Calculations of the Ferroelastic Transition between Rutile-Type and $CaCl_2$-Type SiO_2 at High Pressures. *Phys. Rev. B: Condens. Matter Mater. Phys.* **2008**, *78*, 134106.

(22) Heyd, J.; Scuseria, G. E.; Ernzerhof, M. Hybrid Functionals Based on a Screened Coulomb Potential. *J. Chem. Phys.* **2003**, *118*, 8207−8215.

(23) Krukau, A. V.; Vydrov, O. A.; Izmaylov, A. F.; Scuseria, G. E. Influence of the Exchange Screening Parameter on the Performance of Screened Hybrid Functionals. *J. Chem. Phys.* **2006**, *125*, 224106.

(24) Pickard, C. J.; Needs, R. J. Structure of Phase III of Solid Hydrogen. *Nat. Phys.* **2007**, *3*, 473−476.

(25) Fujihisa, H.; Akahama, Y.; Kawamura, H.; Gotoh, Y.; Yamawaki, H.; Sakashita, M.; Takeya, S.; Honda, K. Incommensurate Composite Crystal Structure of Scandium-II. *Phys. Rev. B: Condens. Matter Mater. Phys.* **2005**, *72*, 132103.

(26) Akahama, Y.; Fujihisa, H.; Kawamura, H. New Helical Chain Structure for Scandium at 240 GPa. *Phys. Rev. Lett.* **2005**, *94*, 195503.

(27) Wang, X.; Chertihin, G. V.; Andrews, L. Matrix Infrared Spectra and DFT Calculations of the Reactive MH_x (x = 1, 2, and 3), $(H_2)MH_2$, MH_2^+, and MH_4^- (M = Sc, Y, and La) Species. *J. Phys. Chem. A* **2002**, *106*, 9213−9225.

(28) Wang, X.; Andrews, L. Homoleptic Tetrahydrometalate Anions MH_4^- (M = Sc, Y, La). Matrix Infrared Spectra and DFT Calculations. *J. Am. Chem. Soc.* **2002**, *124*, 7610−7613.

(29) Ram, R. S.; Bernath, P. F. Fourier Transform Emission Spectroscopy of the $B\ ^1\Pi-X\ ^1\Sigma^+$, $C\ ^1\Sigma^+-X\ ^1\Sigma^+$, and $G\ ^1\Pi-X\ ^1\Sigma^+$ Systems of ScH and ScD. *J. Chem. Phys.* **1996**, *105*, 2668−2674.

(30) Le, A.; Steimle, T. C. Optical Stark Spectroscopy of the $D^1\Pi-X^1\Sigma^+(0,0)$ Band of Scandium Monohydride. *J. Phys. Chem. A* **2011**, *115*, 9370−9376.

(31) Gao, G.; Hoffmann, R.; Ashcroft, N. W.; Liu, H.; Bergara, A.; Ma, Y. Theoretical Study of the Ground-State Structures and Properties of Niobium Hydrides under Pressure. *Phys. Rev. B: Condens. Matter Mater. Phys.* **2013**, *88*, 184104.

(32) Gao, G.; Wang, H.; Zhu, L.; Ma, Y. Pressure-Induced Formation of Noble Metal Hydrides. *J. Phys. Chem. C* **2011**, *116* (2), 1995−2000.

(33) The enthalpy of *Cmcm* is higher than that of $Fm\bar{3}m$ at 250 GPa, though the relative compression ratio of *Cmcm* (2.57) is actually larger than that of $Fm\bar{3}m$ (2.50) at this pressure. A similar case is found in the low-pressure range below 15 GPa, where $P4_2/mmc$ is the most stable phase; however, the relative compression ratio of $Fm\bar{3}m$ is 1.13 larger that that of $P4_2/mmc$ at 1 atm. As in a number of other instances, lower density packings may survive compression (for a while).

(34) Venturini, E. L.; Morosin, B. Low Temperature Anomaly in $Sc_{0.995}Gd_{0.005}H_{1.9}$. *Phys. Lett. A* **1977**, *61*, 326−328.

(35) Merschrod, E. F.; Huang, S. T.; Hoffmann, R. Bonding in an Unusual Nickel Carbide. *Z. Naturforsch.* **1998**, *53B*, 322−332.

(36) Merino, G.; Méndez-Rojas, M. A.; Vela, A.; Heine, T. Recent Advances in Planar Tetracoordinate Carbon Chemistry. *J. Comput. Chem.* **2007**, *28*, 362−372.

(37) Wang, H.; Tse, J. S.; Tanaka, K.; Iitaka, T.; Ma, Y. Superconductive Sodalite-Like Clathrate Calcium Hydride at High Pressures. *Proc. Natl. Acad. Sci. U.S.A.* **2012**, *109*, 6463−6466.

(38) Ye, X. Q.; Luo, D. L.; Luo, L. Z.; Yang, W. C.; Sang, G.; Ao, B. Y.; Huang, H. G.; Tang, T. Effect of Surface Condition on the Kinetics of Scandium-Deuteride Formation. *Vacuum* **2013**, *87*, 40−44.

DOI: 10.1021/jp512538e
J. Phys. Chem. C 2015, 119, 5614−5625

(39) Kong, B.; Zhang, L.; Chen, X. R.; Zeng, T. X.; Cai, L. C. Structural Relative Stabilities and Pressure-Induced Phase Transitions for Lanthanide Trihydrides REH_3 (RE = Sm, Gd, Tb, Dy, Ho, Er, Tm, and Lu). *Phys. B (Amsterdam, Neth.)* **2012**, *407*, 2050−2057.
(40) Kume, T.; Ohura, H.; Takeichi, T.; Ohmura, A.; Machida, A.; Watanuki, T.; Aoki, K.; Sasaki, S.; Shimizu, H.; Takemura, K. High-Pressure Study of ScH_3: Raman, Infrared, and Visible Absorption Spectroscopy. *Phys. Rev. B: Condens. Matter Mater. Phys.* **2011**, *84*, 064132.
(41) In the first to third steps, the c/a ratio was found to be in the range of 1.74−1.80Å; the atomic configuration can be viewed as a distorted hcp form. In later steps, i.e., the fourth or fifth step, the atomic configuration can be viewed as a distorted fcc form. Only in the sixth step does the atomic configuration finally become fcc. In the fourth to sixth steps, c/a has dropped to 1.63−1.66 Å.. The proposed *Cm* structure contains six Sc basal planes, and the β angle is between 108° and 109°.
(42) Segall, M. D.; Philip, J. D. L.; Probert, M. J.; Pickard, C. J.; Hasnip, P. J.; Clark, S. J.; Payne, M. C. First-Principles Simulation: Ideas, Illustrations and the CASTEP Code. *J. Phys.: Condens. Matter* **2002**, *14*, 2717.
(43) Liu, H. Y.; Wang, H.; Ma, Y. M. Quasi-Molecular and Atomic Phases of Dense Solid Hydrogen. *J. Phys. Chem. C* **2012**, *116*, 9221−9226.
(44) A reviewer pointed out to us that the O_h radius of Sc^{3+} (0.885 Å) is not far from that of high spin Fe^{3+} (0.785 Å). Pépin, C. M.; Dewaele, A.; Geneste, G.; Loubeyre, P. New Iron Hydrides under High Pressure. *Phys. Rev. Lett.* **2014**, *113*, 265504. This work characterized some iron hydrides under pressure: FeH ($P6_3/mmc$), FeH_2 ($I4/mmm$), and FeH_3 ($Pm\text{-}3m$). We examined these structural alternatives for ScH, ScH_2, and ScH_3 (see Supporting Information) and found the alternatives less stable for Sc than the structures we have presented.
(45) Zaanen, J.; Sawatzky, G. A.; Allen, J. W. Band Gaps and Electronic Structure of Transition-Metal Compounds. *Phys. Rev. Lett.* **1985**, *55*, 418−421.
(46) Koitzsch, C.; Hayoz, J.; Bovet, M.; Clerc, F.; Despont, L.; Ambrosch-Draxl, C.; Aebi, P. Fermi-Surface Topology of Rare-Earth Dihydrides. *Phys. Rev. B: Condens. Matter Mater. Phys.* **2004**, *70*, 165114.
(47) Yang, J. W.; Gao, T.; Guo, L. Y. *Ab Initio* Study of the Structural, Mechanical, and Dynamical Properties of the Rare-Earth Dihydrides XH_2 (X=Sc, Y, and La). *Phys. B (Amsterdam, Neth.)* **2013**, *429*, 119−126.

Downloaded by CORNELL UNIV on September 8, 2015 | http://pubs.acs.org
Publication Date (Web): February 27, 2015 | doi: 10.1021/jp512538e

DOI: 10.1021/jp512538e
J. Phys. Chem. C 2015, 119, 5614−5625